Title

Advanced schemes for underdense plasma photocathode wakefield accelerators: pathways towards ultrahigh brightness electron beams.

Journal

Philosophical Transactions of the Royal Society A Mathematical Physical and Engineering Sciences, 377(2151)

ISSN

1364-503X

Authors

Manahan, GG
Habib, AF
Scherkl, P
et al.

Publication Date

2019-08-12

DOI

10.1098/rsta.2018.0182

Peer reviewed

PHILOSOPHICAL TRANSACTIONS A

royalsocietypublishing.org/journal/rsta

Review

Cite this article: G. G. Manahan *et al*. 2019 Advanced schemes for underdense plasma photocathode wakefield accelerators: pathways towards ultrahigh brightness electron beams. *Phil. Trans. R. Soc. A* **377**: 20180182.
http://dx.doi.org/10.1098/rsta.2018.0182

Accepted: 18 April 2019

One contribution of 10 to a Theo Murphy meeting issue 'Directions in particle beam-driven plasma wakefield acceleration'.

Subject Areas:
particle physics, plasma physics

Keywords:
plasma wakefield acceleration, underdense plasma photocathode, simultaneous spatial and temporal focusing, energy spread compensation

Author for correspondence:
G. G. Manahan
e-mail: grace.manahan@strath.ac.uk

Advanced schemes for underdense plasma photocathode wakefield accelerators: pathways towards ultrahigh brightness electron beams

G. G. Manahan[1,2], A. F. Habib[1,2], P. Scherkl[1,2], D. Ullmann[1,2], A. Beaton[1,2], A. Sutherland[1,2], G. Kirwan[1,2,3], P. Delinikolas[1,2], T. Heinemann[1,2,3], R. Altuijri[1,2,4], A. Knetsch[3], O. Karger[5], N. M. Cook[6], D. L. Bruhwiler[6], Z.-M. Sheng[1,2,7], J. B. Rosenzweig[8] and B. Hidding[1,2]

[1]Scottish Universities Physics Alliance, Department of Physics, University of Strathclyde, Glasgow G4 0NG, UK
[2]Cockcroft Institute, Sci-Tech Daresbury, Keckwick Lane, Daresbury, Cheshire WA4 4AD, UK
[3]Deutsches Elektronen-Synchrotron DESY, Hamburg, Germany
[4]Physics Department, Princess Nora Bint Abd Ulrahman University, Riyadh, Kingdom of Saudi Arabia
[5]Department of Experimental Physics, University of Hamburg, Hamburg, Germany
[6]RadiaSoft LLC, Boulder, CO, USA
[7]Laboratory for Laser Plasmas and School of Physics and Astronomy, Shanghai Jiao Tong University, Shanghai, People's Republic of China
[8]Particle Beam Physics Laboratory, University of California, Los Angeles, CA, USA

GGM, 0000-0001-5570-3238

The 'Trojan Horse' underdense plasma photocathode scheme applied to electron beam-driven plasma wakefield acceleration has opened up a path which promises high controllability and tunability and to reach extremely good quality as regards emittance and five-dimensional beam brightness. This combination

THE ROYAL SOCIETY PUBLISHING

has the potential to improve the state-of-the-art in accelerator technology significantly. In this paper, we review the basic concepts of the Trojan Horse scheme and present advanced methods for tailoring both the injector laser pulses and the witness electron bunches and combine them with the Trojan Horse scheme. These new approaches will further enhance the beam qualities, such as transverse emittance and longitudinal energy spread, and may allow, for the first time, to produce ultrahigh six-dimensional brightness electron bunches, which is a necessary requirement for driving advanced radiation sources.

This article is part of the Theo Murphy meeting issue 'Directions in particle beam-driven plasma wakefield acceleration'.

1. Introduction

Recently, plasma-based wakefield accelerators, driven by either highly intense laser pulse [1,2] or relativistic electron beams [3,4], are globally seen as the next generation drivers for advanced radiation sources. Their potential applications for high-energy physics are also recognized. This novel acceleration technique can harness high-energy gains in laboratory scale (GV m^{-1}) because the generated plasma waves are capable of sustaining electric fields with amplitudes greater than E_0, the non-relativistic wave breaking field. Mathematically, E_0 can be expressed as $E_0\{\mathrm{V\,m^{-1}}\} \approx 96\sqrt{n_0\{\mathrm{cm^{-3}}\}}$, where n_0 is the background electron density of the plasma [5]. For instance, plasma with a density of $n_0 = 10^{18}\,\mathrm{cm^{-3}}$ can yield accelerating fields of approximately 96 GV m^{-1}—these are orders of magnitude greater than those achievable in conventional RF linacs. Hence, it is possible to realize cost-efficient and medium-scale accelerators. Today, production of quasi-monoenergetic, GeV-scale electron bunches within a few cm accelerating length is routinely demonstrated worldwide [2,4].

In the case of electron beam-driven plasma acceleration (PWFA), electron bunches can be accelerated with high efficiency through the blowout regime, a scenario of highly nonlinear plasma excitation [6,7]. The bunch density, n_b, of the electron beam driver with a bi-Gaussian distribution is described as $n_\mathrm{b} = N_\mathrm{b}/[(2\pi)^{3/2}\sigma_z\sigma_\mathrm{r}^2]$, where N_b is total number of electrons, and σ_z and σ_r are the electron driver's bunch length and radial size. In this highly nonlinear regime, the electron driver bunch density is greater than n_0 ($n_\mathrm{b}/n_0 \gg 1$), such that the plasma electrons are completely expelled, creating a nearly spherical ion cavity, known as the blowout. Furthermore, high-efficient excitation of the blowout is obtained when σ_z is smaller than the plasma wavenumber, k_p [8]. Inside the blowout, strong transverse focusing forces and GV m^{-1} level longitudinal fields are attainable. Hence, various electron injection schemes into this regime have been conceived and studied.

The process of electron injection into the plasma wakes plays a key role because the important beam parameters (such as normalized transverse emittance ε_n, energy spread $\Delta W/W$, total charge Q and bunch duration σ_z) are largely defined by the initial acceleration stage. The various electron bunch injections can be categorized into two: (i) via external injection [3,4] where an electron bunch with an initial energy and beam parameters are injected and further accelerated into a plasma blowout and (ii) via internal injection where the electrons accelerated are initially at rest and the residual transverse momentum is minimal. Example of these internal injection schemes are using plasma density transition [9–12] and those where additional electrons are released within trapping regions based on higher-level ionization due to electron field or wakefield spikes [13–17]. One scheme, known as the underdense plasma photocathode (popularized as the Trojan Horse scheme) is based on ionization injection triggered by a laser pulse. This scheme combines the long acceleration distances of electron beam-driven plasma wakes and limited peak electric fields of particle drivers with the controllability and tunability of the laser pulses to release electrons directly inside the blowout [18,19]. In this method, electron bunches with transverse emittance as low as nm-rad are possible. Therefore, accelerators based on the Trojan Horse scheme may lead to further step-change by increasing the tunability and electron

beam quality in terms of emittance and five-dimensional brightness by orders of magnitude, where the B_{5D} is mathematically expressed as $B_{5D} = 2I_p/\epsilon_n^2$, where I_p is the peak current ($I_p = cQ/\sqrt{2\pi}\sigma_z$). Interestingly, the concept of laser-triggered ionization has also been reported for application in laser wakefield acceleration, which can be found in [20–22] and has shown the production of high-quality electron beams.

In this article, we present an overview of the Trojan Horse scheme, its advantages, challenges and potential applications using the electron bunch generation. We also present advanced and novel methods, which in combination with the Trojan Horse concept aim to enhance the electron beam qualities and, in consequence, will further boost the overall beam brightness.

2. Trojan Horse scheme: the underdense plasma photocathode wakefield acceleration

The Trojan Horse (TH) underdense plasma photocathode scheme requires underdense mixtures of low ionization threshold (LIT) and high-ionization threshold (HIT) species, such as hydrogen and helium (H/He). The high amplitude blowout based on the LIT component is driven by an electron beam, as in the conventional PWFA. Hydrogen, which has ionization thresholds of $\xi_{i,H} = 13.6\,\text{eV}$ for atomic and $\xi_{i,H_2} = 15.4\text{eV}$ for molecular (H_2), is an ideal plasma source because it can be easily ionized either by a modest energy laser pulse or by the self-field of the electron beam driver.

The free electrons are released from the HIT component by a strongly focused, ultra-short laser pulse, which can be called the TH injector laser. Helium is popularly used as a HIT component because of its relative HIT ($\xi_{i,He} = 24.6\,\text{eV}$). The peak amplitude of the normalized vector potential for the laser pulse used to ionize the HIT component can be as low as $a_0 \sim 0.01$. For a linearly polarized Gaussian beam, a_o is related to the laser peak intensity, I_L, as $a_0 \approx 0.85 \times 10^{-9}\lambda\{\mu\text{m}\}\sqrt{I_L\{\text{W cm}^{-2}\}}$, where λ is the laser central wavelength. Here, the laser pulse intensity can be as low as $I_L\{\text{W cm}^{-2}\} = 10^{15}/\lambda^2\{\mu\text{m}\}$ [5]. At these intensities, the oscillating electric fields are sufficient to induce tunnelling ionization [23]. The injected electrons are then rapidly accelerated in the blowout. Because the HIT electrons can be selectively released at any point in the blowout (e.g. at the centre of the blowout, approximately the location of the minimum trapping potential [16]), the trapping requirements are substantially decreased.

Since the wakefield generation and electron bunch injection are completely decoupled in TH scheme, the electron beam production offers more tunability. For instance, multibunches with high beam quality and controlled energies are obtainable with this method. By using synchronized TH injector lasers that are independently tuned, such as by varying the delays and having different foci, electrons are released at different positions inside the plasma blowout, and therefore with different energies [24].

One of the issues in PWFA, particularly in triggered ionization injection schemes, is the occurrence of dark current. Dark current is the result of uncontrollable self-injection of electrons ionized by electric field spikes or 'hot-spots'. These hot spots can be generated by either the (i) wake vertex due to the recombining plasma electrons and/or (ii) by the electron beam driver itself. Detailed studies for the optimization of the electron and plasma dynamics have been carried through in [25] and have obtained conditions for a dark-current free blowout suitable for the TH scheme. Using intensive three-dimensional particle-in-cell (PIC) simulations, it is found that to obtain a dark-current free scenario with TH scheme, a blowout radius must be at all times smaller than the fully pre-ionized plasma column width, otherwise the electrons near this blowout will overshoot and will not be properly re-attracted; therefore the overall blowout dynamics collapses. These have been presented in detail in [25]. Recently, experimental breakthrough and signatures of the TH injection were obtained in the 'E210: Trojan Horse PWFA' program of SLAC FACET-I [26].

In the following sections, we present methods of (i) tailoring the plasma photocathode laser to decrease the release volume of the HIT electrons, which might result in the reduction of the initial

emittance of the electron bunches and (ii) modifying the accelerating fields of the blowout which can result in compensating the accumulated longitudinal energy spread and chirp of the injected electron bunches.

3. Simultaneous spatial and temporal focusing of plasma photocathode laser

In the TH scheme, the reduction in the transverse normalized emittance is a direct consequence of the extremely low residual transverse momentum, $p/m_e c \sim a_0/2$, from the underdense photocathode laser's ponderomotive force. Here, m_e is the electron mass and c is the speed of light. It is furthermore desirable to decrease the release volume of the HIT electrons to reduce both the initial phase space as well as the longitudinal phase mixing due to electrons being born off axis and at different betatron phases of the driving wake [18,27], which can both increase emittance.

One technique to reduce the longitudinal extension of the release region has been reported previously based on the collision of two ultra-short laser pulses in transverse geometry [20]. However, the collision of two lasers creates substantial experimental complexity and challenges in terms of alignment and timing. In this section, we propose the use of simultaneous spatial and temporal focusing (SSTF) of a single laser pulse, a technique known from material processing and microscopy [28–32], and study the applicability for the TH injector lasers. SSTF was first suggested in [33] for a related laser-driven two-pulse scheme. With SSTF combined with TH, it is capable of reducing the release length of the HIT electrons by more than an order of magnitude when compared with the Rayleigh length z_R of a pulse with the typical longitudinal Gaussian distribution.

In the SSTF method, a transverse spatial chirp of the pulse frequency components is generated before passing through a focusing element. This can be done, for example, by placing a single-pass grating pair (suggested by ref. [34]) as sketched in figure 1*a*, where the SSTF configuration is adapted for the TH accelerator. By carefully choosing the arrival time of the SSTF laser with respect to the electron beam driver, the axial peak intensity of the SSTF laser occurs at the centre of the blowout, indicated by the dashed ellipse in figure 1*a*.

The following discussion of SSTF is mainly based on [34], where the analytical study of SSTF is discussed. The spatially chirped laser can be considered analytically as a superposition of Gaussian beamlets, where each beamlet has a radius ($1/e^2$) of $w_{beamlet}$ and is shifted from its central frequency ω_0. If the plasma photocathode laser has an initial spectral bandwidth of $\Delta\omega$, the position of each frequency component is $\alpha\ \Delta\omega$, where α is the chirp rate and can be expressed in the dimensionless parameter as $\beta = \alpha\Delta\omega/w_{beamlet}$ [34]. At the entrance of the focusing element, the transverse profile is elongated along the axis where the chirp is applied due to the lateral stretching of the pulse. The amount of ellipticity can be characterized by a dimensionless parameter called beam aspect ratio, β_{BA}, which is defined as the beam radii ($1/e^2$) ratio of the spatially chirped input pulses. It is expressed as: $\beta_{BA} = \sqrt{1+\beta^2}$ [34]. The frequency components recombine only at the focal region, where the smallest pulse duration is achieved (figure 1*b*). Away from the focus, the pulse is further stretched compared with an unchirped pulse, as shown in figure 1*b*. An initial pulse with symmetric Gaussian distribution, $\lambda = 0.8\,\mu m$, pulse length of $\tau_0 = 40\,fs$ and a focus spot size of $w_0 = 4\,\mu m$, is used for the calculation, giving a Rayleigh length of $z_R = 62\,\mu m$. The structure of an SSTF pulse deviates from a typical Gaussian beam, in which the axial intensity strongly peaks at the focal position and drastically drops farther from the focus, as shown figure 1*c* and figure 2. For $\beta_{BA} = 4$, the FWHM of the axial intensity reduces to $z_{SSTF} \approx 13\,\mu m$, a more than 50% reduction compared to the z_R of the unchirped pulse. If the grating pair can produce spatial chirp with $\beta_{BA} = 14$, z_{SSTF} is further reduced down to 1 µm, more than an order of magnitude smaller than the z_R normally reached by conventional focusing.

It is important to note that the reduction on the FWHM of the axial intensity is primarily β_{BA} dependent, which can be changed by modifying the grating pair set-up. On the other hand, the SSTF pulse maintains its transverse spot size, as shown in figure 1*d*. Here, it is shown that the beam diverges quickly with increasing β_{BA} value; this leads to lower intensities and longer

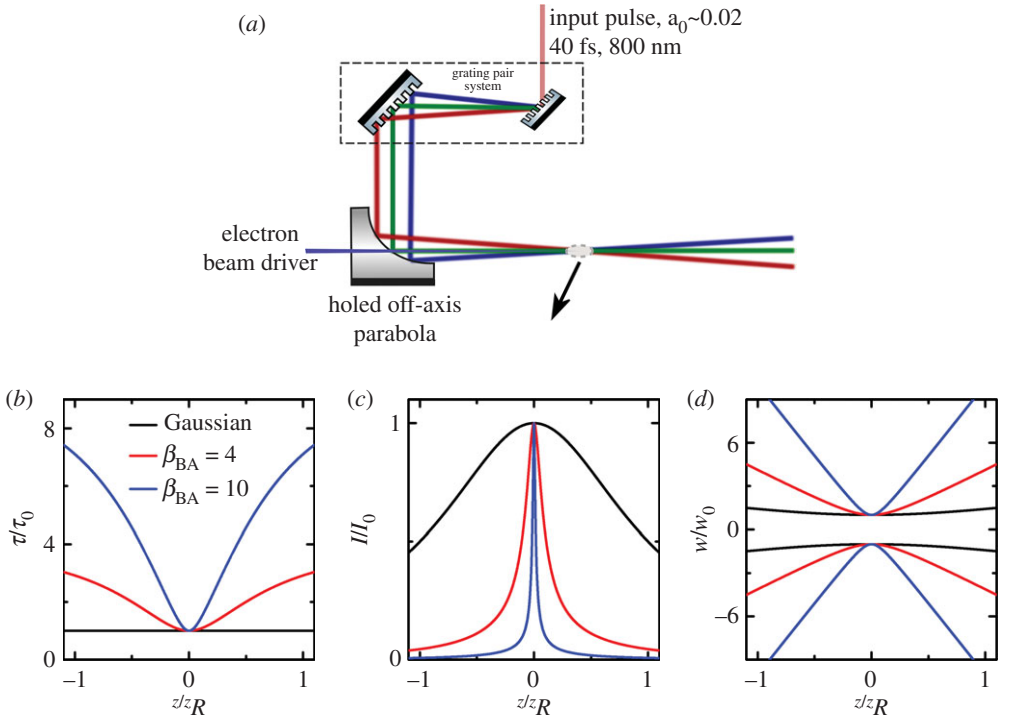

Figure 1. (*a*) Suggested set-up for the SSTF-TH scheme. A spatially chirped laser photocathode is focused at the location of the plasma blowout using an off-axis parabolic mirror. (*b*) Normalized pulse duration τ/τ_0, (*c*) the axial peak intensity I/I_0 and (*d*) transverse beam size w/w_0 of an SSTF pulse as a function of axial position z/z_R for different values of β_{BA}. The parameters are normalized to its corresponding non-spatially chirped pulse with axial Gaussian profile.

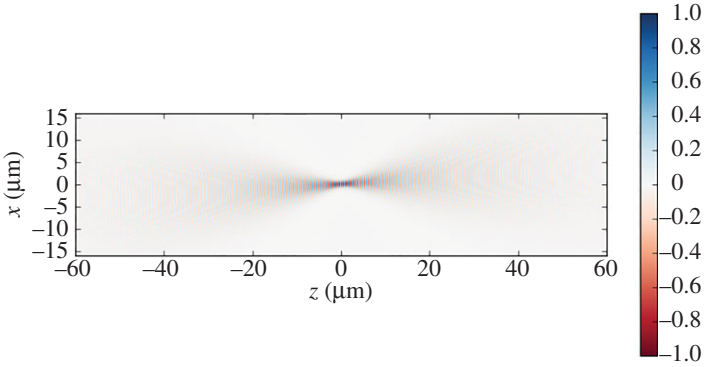

Figure 2. Field propagation of an SSTF pulse with beams aspect ratio of 4. Fields are normalized to 1.

pulse duration far from the focus. These analytical calculations show that with the SSTF method, the axial FWHM of the plasma photocathode laser can be compressed down to 1 µm without significantly changing the peak intensity and spot size. Figure 2 shows the field evolution of an SSTF pulse with a beam aspect ratio of 4, propagating in vacuum. Here, we can see that the fields are only at maximum within a small range of z near the focus location.

As an initial simulation, the SSTF-TH scheme is approximated with VSIM [35] PIC simulations by artificially confining the HIT component in a very narrow region. These are carried through in three dimensions, which is necessary to catch the physics of the bunch generation and trapping

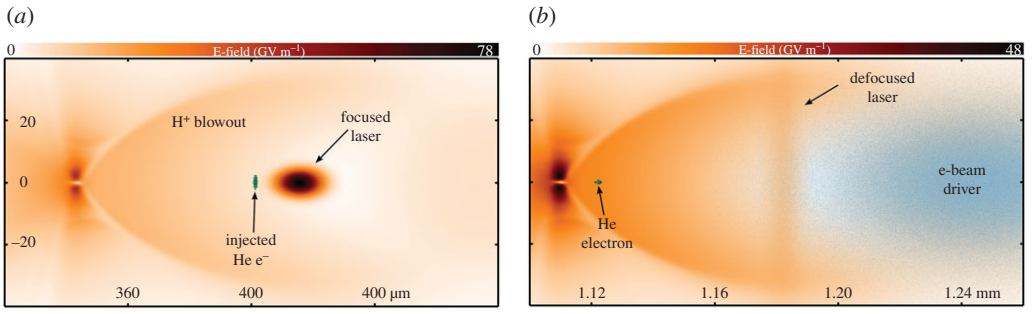

Figure 3. Snapshots from three-dimensional PIC simulation immediately after (*a*) He generation and (*b*) after approximately 1 mm of acceleration.

process adequately. Simulation of longer acceleration distance and parameter scans are also required, which makes the full resolution of the laser pulse resource-prohibitive. Instead, here we rely on analytical estimations of the release region volumes and model the photocathode laser represented using an envelope approximation, propagating collinear and trailing 50 µm behind the electron beam driver. The HIT electron release is triggered by the laser pulse via an advanced tunnelling ionization implementation and is geometrically fully resolved in the transverse direction, but in the axial direction, the release is artificially confined to the corresponding SSTF length as discussed above and plotted in figures 1 and 2. For example, for an SSTF-TH laser with $\beta_{BA} = 14$, $w_0 = 4$ µm and a_0 0.02, the release length is confined to approximately 1 µm longitudinal length. A mixture of hydrogen and helium is used as the LIT/HIT underdense medium. The electron beam driver has the following characteristics: energy $W = 23$ GeV, total charge $Q = 1$ nC, normalized rms emittance $\epsilon_n = 2.25$ µm, rms width $\sigma_r = 20$ µm and rms length $\sigma_z = 30$ μm, corresponding to a bunch density $n_b \approx 2 \times 10^{17}$ cm^{-3}. The hydrogen component is pre-ionized at a density of $n_H = 5 \times 10^{16}$ cm^{-3}, corresponding to a plasma wavelength $\lambda_p = \sqrt{\pi / n_H r_e} \approx$ 150 µm, where r_e is the classical radius of an electron, while the He density is maintained to $n_H = 5 \times 10^{17}$ cm^{-3}.

Figure 3*a*,*b* shows the wake driven by the electron beam immediately after when He electrons are (a) generated by an approximately 40 fs laser pulse inside the blowout at the focal region (equivalent to the longitudinal distance of $z = 400$ µm) and are (b) trapped and accelerated after 1 mm, where the bunch has gained a maximum energy of 10 MeV. In contrast to conventional TH, where the initial bunch distribution is rather cigar-like, since $z_R > w_0$, in SSTF-TH, the initial bunch distribution is pancake-like, since $z_{SSTF} < w_0$. This can be seen in figure 3*a*. From the initial results, the rms transverse emittance of the witness bunch using this SSTF approximation produces lower rms transverse emittance by an order of magnitude, as compared with the usual TH pulse that has Gaussian distribution. Note that the artificial confinement of the SSTF in these simulations is implemented because SSTF is a spatial chirp and thus the bandwidth of the laser pulse changes through the propagation axis. Since we are using an envelope approximation in VSIM, the effect of the bandwidth on the dispersion of each frequency component of the laser in the plasma is not implemented. The consideration of the SSTF pulse dispersion in plasma is currently ongoing and will be discussed elsewhere.

4. Compact, plasma-based energy compensation technique

The high-energy acceleration in plasma inherently produces electron bunches with substantial longitudinal energy spread or chirp. This is well-known and is, currently, the central challenge in any plasma-based accelerators. The large energy spread is detrimental in several ways. Beam extraction and transport is difficult and leads to deterioration of the transverse emittance. It also limits the applications of these beams for advanced radiation sources. Therefore, the 'energy

spread and chirp problem' degrades the overall beam brightness and is a showstopper for fully harnessing the potentials of plasma-based accelerators.

Conventionally, six-dimensional beam brightness is a figure of merit for comparing the quality of the radiation sources. High six-dimensional brightness beams are characterized by high peak current, low transverse normalized emittance and narrow longitudinal energy spread. It is essential in many applications, such as to reach high-gain and shorter wavelengths in free-electron lasers [36] and for high-energy colliders, to enhance the focusability of the beam and increase its luminosity [37]. The six-dimensional beam brightness can be expressed mathematically as $B_{6D} = B_{5D}/0.1\%\Delta W_{\mathrm{rms}}/W\{\mathrm{Am}^{-1}/0.1\ \mathrm{BW}\}$.

In this section, a flexible scheme of tailoring the energy distribution of low-emittance electron beams inside a plasma-based accelerator is discussed, a concept which is initially introduced in [38]. The tailoring process is based on the beam-loading mechanism and can be tuned to achieve energy spread reduction without altering the electron beam emittance. In this concept, two moderate TH laser pulses are used to inject electrons into the accelerating plasma wake and modify the field so that the accelerated low-emittance electron beam of interest (called the witness bunch) will experience a longitudinal phase space rotation. This idea is one of the applications of the electron multibunch production as mentioned in §2. The loaded field reverses the effective accelerating gradient and counter-rotates the accumulated longitudinal energy spread of the witness bunch. As a result, the energy spread is reduced, enabling the production of ultrahigh six-dimensional brightness beams.

In this concept of plasma dechirper, the first TH laser releases the witness bunch at the beginning of the plasma stage. The parameters of the first TH laser are typical for any TH scheme, i.e. $a_0 \ll 1$ and strongly focus, e.g. spot size $w_0 < 5\,\mu\mathrm{m}$. This ensures that the injected electrons will have good beam qualities. After a period of acceleration, in which the witness bunch has gained sufficient energy and is stabilized, a second TH laser is introduced and this laser releases a second batch of electrons, which is called in ref. [38] the 'escort bunch.' The parameters ($a_{0,}$ w_{o} and τ_0) of the second TH laser pulse are considerably higher than the first TH laser, such that the produced escort bunch will have a bunch charge density that is capable of overloading the wakefield. In [38], the escort bunch has gained a total charge of 100 pC in comparison to the witness bunch that is only 5 pC and has shown that it significantly alters the longitudinal electric field. That means that the presence of the escort bunch strongly overloads the electric field. This results in the counter-clockwise rotation of the longitudinal phase space of the witness bunch while further accelerating it. As a consequence, the correlated energy spread is reduced to its minimum value, a position where extraction is ideal. The resulting energy compensation is shown in figure 4, in which the phase space of the witness bunch at the position of the minimum energy spread is plotted. The extent of the overloaded field, known as the 'dechirping region,' must be much longer than the witness bunch such that the dechirping occurs from head to tail of the bunch. That means that the optimization of the escort bunch must be focused on obtaining high charge and longer bunch duration than the witness bunch.

The main challenges of this approach are the additional laser pulse to produce the escort bunch and the tunability and spatio-temporal alignment accuracy of both laser pulses. To test how the alignment of the two TH laser pulses affects the plasma dechirping process, an initial jitter study is performed. For this analysis, the first TH laser is introduced with a transverse offset with respect to the blowout axis. The result is shown in figure 5, where the dechirping distance, Δz, and the resulting uncorrelated energy spread are monitored. In this study, a comparable shorter plasma wavelength ($\lambda_{\mathrm{p}} \sim 100\,\mu\mathrm{m}$) is used, corresponding to a blowout radius, $R_{\mathrm{b,max}} = 40\,\mu\mathrm{m}$. As shown in the plot, the dechirping distance and residual energy spread of the witness bunch is quite resilient to the jitter of the initial position of the first TH laser pulse, ie. the y-offset must be greater than $0.2{*}R_{\mathrm{b,max}}$ to see a significant increase in the uncorrelated energy spread. Fortunately, the tolerance against spatio-temporal alignment jitters increases when considering longer plasma wavelengths (hence smaller plasma densities). This is because the plasma blowout increases both in the longitudinal and transverse direction. The laser-to-electron drive beam jitter, however, is independent of the plasma wavelength, which means that at lower plasma densities,

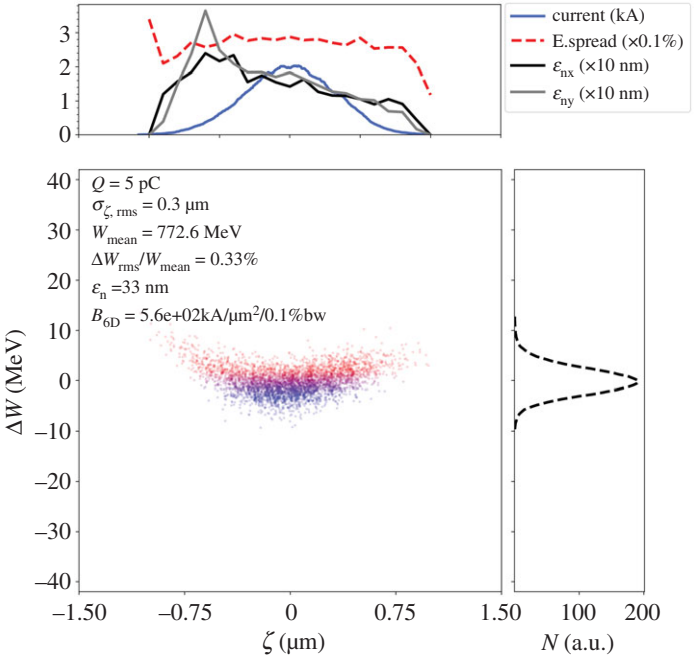

Figure 4. Longitudinal phase space of the witness bunch during at the position of minimum energy spread from ref. [38].

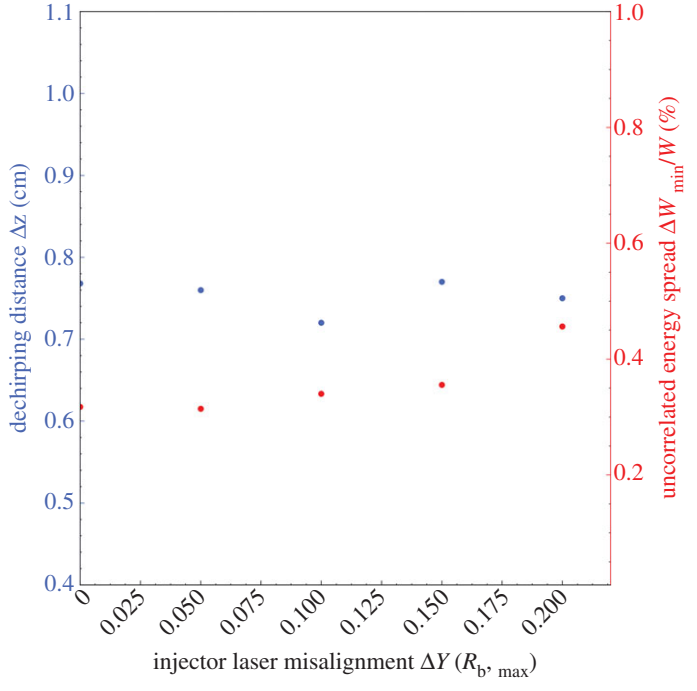

Figure 5. Effect of the first TH laser pulse offset to the plasma-based dechirping techniques. The initial position of TH laser is offset transversely with respect to the blowout axis. Here, the plasma wavelength is 100 μm, thereby the maximum blowout radius, $R_{b,max}$, is 40 μm.

it is easier to release the electrons consistently in the desired phase and at the right trapping position. Furthermore, the residual uncorrelated energy spread decreases when going to longer plasma wavelengths.

5. Conclusion

In this paper, the Trojan Horse scheme is reviewed for its application in electron beam-driven plasma wakefield accelerator. The decoupling of the plasma blowout generation and electron injection allows greater tunability and control of the acceleration process and witness bunch qualities, such as transverse emittance and five-dimensional brightness. These developments in electron beam emittance and five-dimensional-brightness may have a transformative impact on key applications such as compact yet high-performance free-electron lasers. Two advanced methods were presented and were proposed to integrate with the TH scheme. These combinations have the potential of further improving the witness bunch qualities and may pave the way of boosting the six-dimensional beam brightness of the electron bunches.

Data accessibility. Data are available upon request through the corresponding author.

Authors' contributions. All authors contributed equally to this manuscript.

Competing interests. We declare we have no competing interests.

Funding. This work used computational resources of the National Energy Research Scientific Computing Center, which is supported by DOE DE-AC02-05CH11231, and of JURECA (project no. hhh36), of HLRN, and Shaheen (project no. k1191), and the DFG Emmy-Noether program. This work was supported by a fellowship within the FIT worldwide programme of the German Academic Exchange Service (DAAD) and by RadiaBeam Technologies. N.M.C. and D.L.B. would like to acknowledge DOE Office of Science award no. DE-SC0013855.

Acknowledgement. We acknowledge the in-depth discussion of SSTF application to TH scheme with R. Lehe and S. Hooker.

References

1. Wang X *et al.* 2013 Quasi-monoenergetic laser-plasma acceleration of electrons to 2 GeV. *Nat. Commun.* **4**, 1988. (doi:10.1038/ncomms2988)
2. Leemans WP *et al.* 2014 Multi-GeV electron beams from capillary-discharge-guided subpetawatt laser pulses in the self-trapping regime. *Phys. Rev. Lett.* **113**, 245002. (doi:10.1103/PhysRevLett.113.245002)
3. Blumenfeld I *et al.* 2007 Energy doubling of 42 GeV electrons in a metre-scale plasma wakefield accelerator. *Nature* **445**, 741–744. (doi:10.1038/nature05538)
4. Litos M *et al.* 2014 High-efficiency acceleration of an electron beam in a plasma wakefield accelerator. *Nature* **515**, 92–95. (doi:10.1038/nature13882)
5. Esarey E, Schroeder CB, Leemans W. 2009 Physics of laser-driven plasma-based electron accelerators. *Rev. Mod. Phys.* **81**, 1229. (doi:10.1103/RevModPhys.81.1229)
6. Rosenzweig JB, Breizman B, Katsouleas T, Su JJ. 1991 Acceleration and focusing of electrons in two-dimensional nonlinear plasma wakefields. *Phys. Rev. A* **44**, R6189–R6192. (doi:10.1103/PhysRevA.44.R6189)
7. Lu W, Huang C, Zhou M, Mori WB, Katsouleas T. 2006 Nonlinear theory for relativistic plasam wakefields in the blowout regime. *Phys. Rev. Lett.* **96**, 165002. (doi:10.1103/PhysRevLett.96.165002)
8. Barov N, Rosenzweig JB, Thompson MC, Yoder RB. 2004 Energy loss of a high-charge bunched electron beam in plasma: analysis. *Phys. Rev. Accel. Beams.* **7**, 061301. (doi:10.1103/PhysRevSTAB.7.061301)
9. Suk H, Barov N, Rosenzweig JB, Esarey E. 2001 Plasma electron trapping and acceleration in a plasma wake field using a density transition. *Phys. Rev. Lett.* **86**, 1011–1014. (doi:10.1103/PhysRevLett.86.1011)
10. Geddes CGR, Nakamura K, Plateau GR, Toth C, Cormier-Michel E, Esarey E, Schroeder CB, Cary JR, Leemans WP. 2008 Plasma-density gradient injection of low absolute momentum spread electron bunches. *Phys. Rev. Lett.* **100**, 215004. (doi:10.1103/PhysRevLett.100.215004)

11. Bulanov S, Naumova N, Pegoraro F, Sakai J. 1998.Particle injection into the wave acceleration phase due to nonlinear wave wake breaking. *Phys. Rev. E.* **58**, R5257–R5260. (doi:10.1103/PhysRevE.58.R5257)
12. Xu XL, Li F, An W, Dalichaouch TN, Yu P, Lu W, Joshi C, Mori WB. 2017 High quality electron bunch generation using a longitudinal density-tailored plasma-based accelerator in the three-dimensional blowout regime. *Phys. Rev. Accel. Beams.* **20**, 111303. (doi:10.1103/PhysRevAccelBeams.20.111303)
13. Umstadter D, Kim JK, Dodd E. 1995 Method and apparatus for generating and accelerating ultrashort pulses. US Patent Serial No. 5789876.
14. Chen M, Sheng Z-M, Ma Y-Y, Zhang J. 2006 Electron injection and trapping in a laser wakefield by field ionization to high-charge states of gases. *Journ. Applied Phys.* **99**, 056109. (doi:10.1063/1.2179194)
15. Oz E *et al.* 2007 Ionization-induced electron trapping in ultrarelativistic plasma wakes. *Phys. Rev. Lett.* **98**, 084801. (doi:10.1103/PhysRevLett.98.084801)
16. Pak A, Marsh KA, Martins SF, Lu W, Mori WB, Joshi C. 2010 Injection and trapping of tunnel-ionized electrons into laser-produced wakes. *Phys. Rev. Lett.* **104**, 025003. (doi:10.1103/PhysRevLett.104.025003)
17. Martinez de la Ossa A, Grebenyuk J, Mehrling T, Schaper L, Osterhoff J. 2013 High-quality electron beams from beam-driven plasma accelerators by wakefield-induced ionization injection. *Phys. Rev. Lett.* **111**, 245003. (doi:10.1103/PhysRevLett.111.245003)
18. Hidding B, Pretzler G, Rosenzweig JB, Königstein T, Schiller D, Bruhwiler DL. 2012 Ultracold electron bunch generation via plasma photocathode emission and acceleration in a beam-driven plasma blowout. *Phys. Rev. Lett.* **108**, 035001. (doi:10.1103/PhysRevLett.108.035001)
19. Xi Y, Hidding B, Bruhwiler D, Pretzler G, Rosenzweig JB. 2013 Hybrid modeling of relativistic underdense plasma photocathode injectors. *Phys. Rev. ST Accel. Beams.* **16**, 031303. (doi:10.1103/PhysRevSTAB.16.031303)
20. Li F *et al.* 2013 Generating high-brightness electron beams via ionization injection by transverse colliding lasers in plasma-wakefield accelerator. *Phys. Rev. Lett.* **111**, 015003. (doi:10.1103/PhysRevLett.111.015003)
21. Yu LL, Esarey E, Schroeder CB, Vay J-L, Benedetti C, Geddes CR, Chen M, Leemans WP. 2014 Two-color laser ionization injection. *Phys. Rev. Lett.* **112**, 125001. (doi:10.1103/PhysRevLett.112.125001)
22. Xu XL *et al.* 2016 Nanoscale electron bunching in laser-triggered ionization injection in plasma accelerators. *Phys. Rev. Lett.* **117**, 034801. (doi:10.1103/PhysRevLett.117.034801)
23. Chen M, Cormier-Michel E, Geddes CGR, Bruhwiler DL, Yu LL, Esarey E, Schroeder CB, Leemans WP. 2013 Numerical modeling of laser tunnelling ionization in explicit particle-in-cell codes. *Journ. Comp. Phys.* **236**, 220–228. (doi:10.1016/j.jcp.2012.11.029)
24. Hidding B *et al.* 2014 Tunable electron multibunch production in plasma wakefield accelerators. arXiv:1403.1109
25. Manahan GG *et al.* 2016 Hot spots and dark current in advanced plasma wakefield accelerators. *Phys. Rev. Accel. Beams.* **19**, 011303. (doi:10.1103/PhysRevAccelBeams.19.011303)
26. Hidding B *et al.* 2017. First measurements of Trojan Horse injection in a plasma wakefield accelerator. *Proc. of IPAC* **2017**, 1252–1257.
27. Xu XL *et al.* 2014 Phase-space dynamics of ionization injection in plasma-based accelerators. *Phys. Rev. Lett.* **112**, 035003. (doi:10.1103/PhysRevLett.112.035003)
28. Oron D, Tal E, Silberberg Y. 2005 Scanningless depth-resolved microscopy. *Opt. Exp.* **13**, 1468. (doi:10.1364/OPEX.13.001468)
29. Durst ME, Zhu G, Xu C. 2006 Simultaneous spatial and temporal focusing for axial scanning. *Opt. Exp.* **14**, 12 243–12 254. (doi:10.1364/OE.14.012243)
30. Durst ME, Zhu G, Xu C. 2007 Simultaneous spatial and temporal focusing in nonlinear microscopy. *Opt. Commun.* **281**, 1796–1805. (doi:10.1016/j.optcom.2007.05.071)
31. Block E, Greco M, Vitek D, Masihzadeh O, Ammar DA, Kahook MY, Mandava N, Durfee C, Squier J. 2013 Simultaneous spatial and temporal focusing for tissue ablation. *Biomed. Opt. Exp.* **4**, 831–841. (doi:10.1364/BOE.4.000831)
32. Kammel R, Ackermann R, Thomas J, Götte J, Skupin S, Tünnermann A, Nolte S. 2014 Enhancing precision in fs-laser material processing by simultaneous spatial and temporal focusing. *Light Sci. Appl.* **3**, e169. (doi:10.1038/lsa.2014.50)

33. Bourgeois N, Cowley J, Hooker SM. 2013 Two-pulse ionization injection into quasilinear laser wakefields. *Phys. Rev. Lett.* **111**, 155004. (doi:10.1103/PhysRevLett.111.155004)
34. Durfee CG, Greco M, Block E, Vitek D, Squier JA. 2012 Intuitive analysis of space-time focusing with double-ABCD calculation. *Opt. Exp.* **20**, 14244. (doi:10.1364/OE.20.014244)
35. Nieter C, Cary JR. 2004 VORPAL: a versatile plasma simulation code. *J. Comp. Phys.* **196**, 448–478. (doi:10.1016/j.jcp.2003.11.004)
36. Di Mitri S. 2015 On the importance of electron beam brightness in high gain free electron lasers. *Photonics* **2**, 317–341. (doi:10.3390/photonics2020317)
37. Emma P, Raubenhemier T. 2001 Systematic approach to damping ring design. *Phys. Rev. Accel. Beams* **4**, 021001. (doi:10.1103/PhysRevSTAB.4.021001)
38. Manahan GG *et al.* 2017 Single-stage plasma-based correlated energy spread compensation for ultrahigh 6D brightness electron beams. *Nat. Commun.* **8**, 15705. (doi:10.1038/ncomms15705)